Cellular/Molecular

A Selective Glial Barrier at Motor Axon Exit Points Prevents Oligodendrocyte Migration from the Spinal Cord

Sarah Kucenas,[1,2] Wen-Der Wang,[2,3] Ela W. Knapik,[2,3] and Bruce Appel[1,4]

[1]Department of Biological Sciences, [2]Vanderbilt Program in Developmental Biology, and [3]Division of Genetic Medicine, Vanderbilt University, Nashville, Tennessee, 37235, and [4]Department of Pediatrics, University of Colorado Denver–Anschutz Medical Campus, Aurora, Colorado 80045

Nerve roots have specialized transition zones that permit axon extension but limit cell movement between the CNS and PNS. Boundary cap cells prevent motor neuron soma from following their axons into the periphery, thereby contributing to a selective barrier. Transition zones also restrict movement of glial cells. Consequently, axons that cross the CNS–PNS interface are insulated by central and peripheral myelin. The mechanisms that prevent the migratory progenitors of oligodendrocytes and Schwann cells, the myelinating cells of the CNS and PNS, respectively, from crossing transition zones are not known. Here, we show that interactions between myelinating glial cells prevent their movements across the interface. Using *in vivo* time-lapse imaging in zebrafish we found that, in the absence of Schwann cells, oligodendrocyte progenitors cross ventral root transition zones and myelinate motor axons. These studies reveal that distinct mechanisms regulate the movement of axons, neurons, and glial cells across the CNS–PNS interface.

Introduction

Communication between CNS and peripheral nervous system (PNS) occurs via regularly spaced nerve roots where axons either cross into or out of the neuraxis. In rodent and bird embryos, neural crest-derived cells are tightly associated with the end feet of radial glia and astrocytes at axon entry and exit points, disrupting the basal lamina that covers the spinal cord and brain (Altman and Bayer, 1984; Golding and Cohen, 1997; Fraher et al., 2007). Interaction of neural crest cells with radial glia and astrocytes might contribute to a selective gating mechanism that permits axon crossing but not neuronal migration, thereby maintaining the integrity of the CNS–PNS interface.

Axon entry and exit points are also the sites of a transition between central and peripheral myelin. Oligodendrocytes and Schwann cells, the myelinating glia of the CNS and PNS, respectively, form unique heminodes on axons precisely at the interface (Fraher and Kaar, 1984; Fraher, 2000). Oligodendrocyte and Schwann cell progenitors are highly migratory (Kalderon, 1979; Bhattacharyya et al., 1994; Kirby et al., 2006) and Schwann cells can invade the CNS following injury (Gilmore and Sims, 1997). However, the presence of Schwann cells in the CNS and oligodendrocytes in the periphery of normal animals is rare (Maxwell et al., 1969; Raine, 1976; Jung et al., 1978). The mechanisms that establish boundaries between different myelinating cells and prevent oligodendrocytes and Schwann cells from crossing the CNS–PNS interface during normal development are not known.

We recently described a population of ventral spinal cord glial cells in zebrafish that migrate through motor axon exit points (MEPs) and develop as perineurial cells, which tightly wrap and protect peripheral nerves (Kucenas et al., 2008). This raised the possibility that axon entry and exit points regulate the movement of glial cells as well as axons and neurons. To test this we performed time-lapse imaging experiments to follow glial cell movements in zebrafish embryos and larvae. These studies revealed that, in the absence of Schwann cells, oligodendrocyte progenitor cells (OPCs) migrate through MEPs and myelinate peripheral motor axons. Therefore, distinct and highly selective gating mechanisms regulate the movement of axons, neurons, and glia across the boundary separating the CNS and PNS.

Materials and Methods

Fish husbandry. All animal studies were approved by Vanderbilt University Institutional Animal Care and Use Committee. Zebrafish strains used in this study included AB, *Tg(nkx2.2a:megfp)^{vu17}* (Kirby et al., 2006; Kucenas et al., 2008b), *Tg(sox10(7.2):mrfp)^{vu234}* (Kucenas et al., 2008b), *Tg(olig2:egfp)^{vu12}* (Shin et al., 2003), *colourless(cls)^{m241}* (Dutton et al., 2001), *mont blanc(mob)^{m610}*, and *mother superior(mos)^{m188}* (Neuhauss et al., 1996). Embryos were produced by pairwise matings, raised at 28.5°C in egg water or embryo medium and staged according to hours postfertilization (hpf). Embryos used for *in situ* hybridization, immunocytochemistry, and microscopy were treated with 0.003% phenylthiourea in egg water to reduce pigmentation.

In vivo *imaging.* At 24 hpf, all embryos used for live imaging were manually dechorionated and transferred to egg water containing phenylthiourea. At specified stages, embryos were anesthetized using 3-aminobenzoic acid ester (Tricaine), immersed in 0.8% low-melting point agarose, and mounted on their sides in glass-bottomed 35 mm Petri

Received Aug. 24, 2009; revised Oct. 9, 2009; accepted Oct. 19, 2009.

This work was supported by National Institutes of Health (NIH) Ruth L. Kirschstein National Research Service Award HD056760 (S.K.), NIH Grant NS046668 (B.A.), NIH Grant DE18477 (E.K), and a zebrafish initiative funded by the Vanderbilt University Academic Venture Capital Fund. We thank members of the Appel laboratory for valuable discussions and Jonathon Gitlin for comments on the manuscript. The anti-Isl antibody, developed by T. M. Jessell, was obtained from the Developmental Studies Hybridoma Bank developed under the auspices of the National Institute of Child Health and Human Development and maintained by The University of Iowa, Department of Biological Sciences, Iowa City, IA 52242.

Correspondence should be addressed to Bruce Appel, Department of Pediatrics, University of Colorado Denver–Anschutz Medical Campus, Mail Stop 8108, Aurora, Colorado 80045. E-mail: Bruce.Appel@ucdenver.edu.

S. Kucenas' present address: Department of Biology, University of Virginia, Charlottesville, VA 22904-4328.

DOI:10.1523/JNEUROSCI.4193-09.2009

 0270-6474/09/2915187-08$15.00/0

dishes (World Precision Instruments). All images were captured using a 40× oil-immersion objective (numerical aperture = 1.3) mounted on a motorized Zeiss Axiovert 200 microscope equipped with a PerkinElmer ERS spinning-disk confocal system. During time-lapse experiments, a heated stage chamber was used to maintain embryos at 28.5°C. Z image stacks were collected every 10–15 min, and three-dimensional datasets were complied using Sorenson 3 video compression (Sorenson Media) and exported to QuickTime (Apple) to create movies.

In situ *RNA hybridization.* Embryos and larvae were fixed in 4% paraformaldehyde for 24 h, stored in 100% methanol at −20°C, and processed for *in situ* RNA hybridization. Plasmids were linearized with appropriate restriction enzymes and cRNA preparation was performed using Roche DIG-labeling reagents and T3, T7 or SP6 RNA polymerases (New England Biolabs). After the *in situ* hybridization, embryos were embedded in 1.5% agar/30% sucrose and frozen in 2-methyl butane chilled by immersion in liquid nitrogen. Transverse sections (10 μm) were collected on microscope slides using a cryostat microtome and covered with 75% glycerol. Images were obtained using a Retiga Exi-cooled CCD camera (Qimaging) mounted on an Olympus AX70 microscope equipped with Openlab software (Improvision). All images were imported into Adobe Photoshop. Adjustments were limited to levels, contrast, color matching settings, and cropping.

Immunohistochemistry. Embryos and larvae were fixed in AB Fix (4% paraformaldehyde, 8% sucrose, 1× PBS) for 3 h at 23°C or overnight at 4°C and embedded as described above. We collected 10 μm transverse sections using a cryostat microtome. Sections were rehydrated in 1× PBS for 60 min at 23°C and preblocked in 2% goat serum/BSA/1× PBS for 30 min. Sections were incubated in primary antibody overnight at 4°C. The primary antibodies used included mouse anti-Isl (39.4D5, 1:100; Developmental Studies Hybridoma Bank), rabbit antibody to Sox10 (Park et al., 2005) (1:500), rabbit antibody to MBP (1:500, generated commercially against the peptide sequence CSRSRSPPKRWSTIF, Open Biosystems), and mouse antibody to acetylated tubulin (1:5000, Sigma). Sections were washed extensively with 1× PBS, incubated for 3 h at 23°C with either Alexa Fluor 647 goat anti-rabbit or Alexa Fluor 568 goat anti-mouse (Invitrogen) as secondary antibodies for detection of primary antibodies, and washed with 1× PBS for 30 min. Sections were mounted in Vectashield (Vector Laboratories) and imaged using the confocal microscope described above. Image adjustments were limited to contrast enhancement and levels settings using Volocity software (Improvision) and Adobe Photoshop.

Electron microscopy. 5 days postfertilization (dpf) larvae were killed with Tricaine, fixed in 4% glutaraldehyde in 0.05 M PBS-Sucrose for 1 h, washed three times in dH_2O and placed into fresh 4% glutaraldehyde overnight. Samples were postfixed in 2% OsO_4 in 0.1 M PBS-Sucrose for 2 h at 23°C, washed three times in dH_2O, and stained in uranyl acetate for 2 h to enhance contrast. Samples were then subjected to complete dehydration in an ethanol series: 50%, 70%, 95%, 100% ethanol three times for 15 min each, and processed with 100% propylene oxide three times for 15 min. Samples were subsequently equilibrated in 50% epon/50% propylene oxide overnight at 23°C, transferred to fresh 100% epon for 6 h, and then placed in a 65°C vacuum oven overnight to facilitate infiltration of the tissue. Ultrathin section (70–90 nm) were obtained on a Leica UCT Ultracut microtome, transferred to copper grids and examined on a Phillips CM12 TEM equipped with a high resolution CCD digital camera.

Data quantification and statistical analysis. To count cells in mutant and wild-type larvae, composite Z image stacks were compiled using Volocity software. Cell counts were taken from lateral, whole-mount views between somites 8 and 13. Individual z images were sequentially observed and cells counted within the entire z stack. All graphically presented data represents the mean of the analyzed data. Statistical analyses were performed with Prism software. The level of significance was determined by either paired or unpaired *t* tests using a confidence interval of 95%.

Results

OPCs migrate from the spinal cord to replace Schwann cells along spinal motor nerves

To test the hypothesis that interactions between myelinating cells influence their distribution and behaviors at transition zones, we performed time-lapse imaging of zebrafish embryos and larvae carrying mutations that disrupt Schwann cell development. We first examined *colourless* (*cls*) mutant embryos, which are deficient for Sox10 function and lack differentiated Schwann cells (Dutton et al., 2001). To follow the glial cells, we created *cls*$^{-/-}$*; Tg(olig2:egfp);Tg(sox10(7.2):mrfp)* embryos, in which both OPCs and Schwann cells express membrane-tethered red fluorescent protein (RFP) under control of *sox10* regulatory DNA (Kucenas et al., 2008) and OPCs but not Schwann cells express cytosolic enhanced green fluorescent protein (EGFP) (Shin et al., 2003), thereby allowing us to easily distinguish between these cell types. Time-lapse imaging revealed that Schwann cells migrated to motor roots but failed to wrap axons (Fig. 1; supplemental Movie 1, available at www.jneurosci.org as supplemental material). At the same time, long processes of cells marked by EGFP and RFP, indicative of OPCs, began to emerge from the spinal cord at MEPs. These processes sometimes appeared to contact Schwann cells while their cell bodies remained within the spinal cord. Eventually, Schwann cells fragmented and died. Immediately afterward, EGFP$^+$ RFP$^+$ OPCs migrated from the spinal cord through MEPs. OPC migration through MEPs began ~12 h after OPC specification in the spinal cord and occurred at every motor root, but only after Schwann cells died. Peripheral OPCs had morphologies and behaviors similar to central OPCs (Kirby et al., 2006), extending and retracting long membrane processes and sometimes dividing. Despite remaining associated with motor roots, peripheral OPCs did not wrap axons and eventually died. OPCs that remain within the spinal cord of *cls* mutant larvae initiate axon wrapping before dying (N. Takada, S. Kucenas, and B. Appel, unpublished observations).

Because both Schwann cells and OPCs require Sox10 function, we sought a second method for eliminating Schwann cells that would not affect OPC development. Embryos that are homozygous for mutations of *mont blanc (mob)* and *mother superior (mos)*, which disrupt functions of the Tfap2a and Foxd3 transcription factors, respectively (Barrallo-Gimeno et al., 2004; Montero-Balaguer et al., 2006), do not have neural crest derivatives and, consequently, do not have Schwann cells (Arduini et al., 2009) (Wang et al., in preparation). Nevertheless, we found that *mob*$^{-/-}$*;mos*$^{-/-}$ larvae had Sox10$^+$ cells associated with motor roots (Fig. 2*D*,*E*). Although mutant larvae had far fewer ventral root-associated Sox10$^+$ cells than wild type, the number increased slightly to ~3 cells per root between 3 and 4 dpf (Fig. 2*G*). In contrast, the lateral line nerves, which are myelinated by Sox10$^+$ Schwann cells in wild-type larvae, had no Sox10$^+$ cells associated with them in *mob*$^{-/-}$*;mos*$^{-/-}$ larvae (data not shown).

To verify our observation that OPCs occupy motor nerves in the absence of Schwann cells in *mob*$^{-/-}$*;mos*$^{-/-}$ larvae and further document their behaviors, we performed additional time-lapse imaging. In the following experiments we imaged a total of 11 mutant larvae, analyzing 3 motor roots per larva, and observed consistent behaviors at each root. Combination of the *Tg(nkx2.2a:megfp)* and *Tg(sox10(7.2)mrfp)* transgenes creates a color code whereby Schwann cells are red (*nkx2.2a*$^-$ *sox10*$^+$), perineurial glia are green (*nkx2.2a*$^+$ *sox10*$^-$), and OPCs are red or yellow because zebrafish *sox10*$^+$ OPCs are either

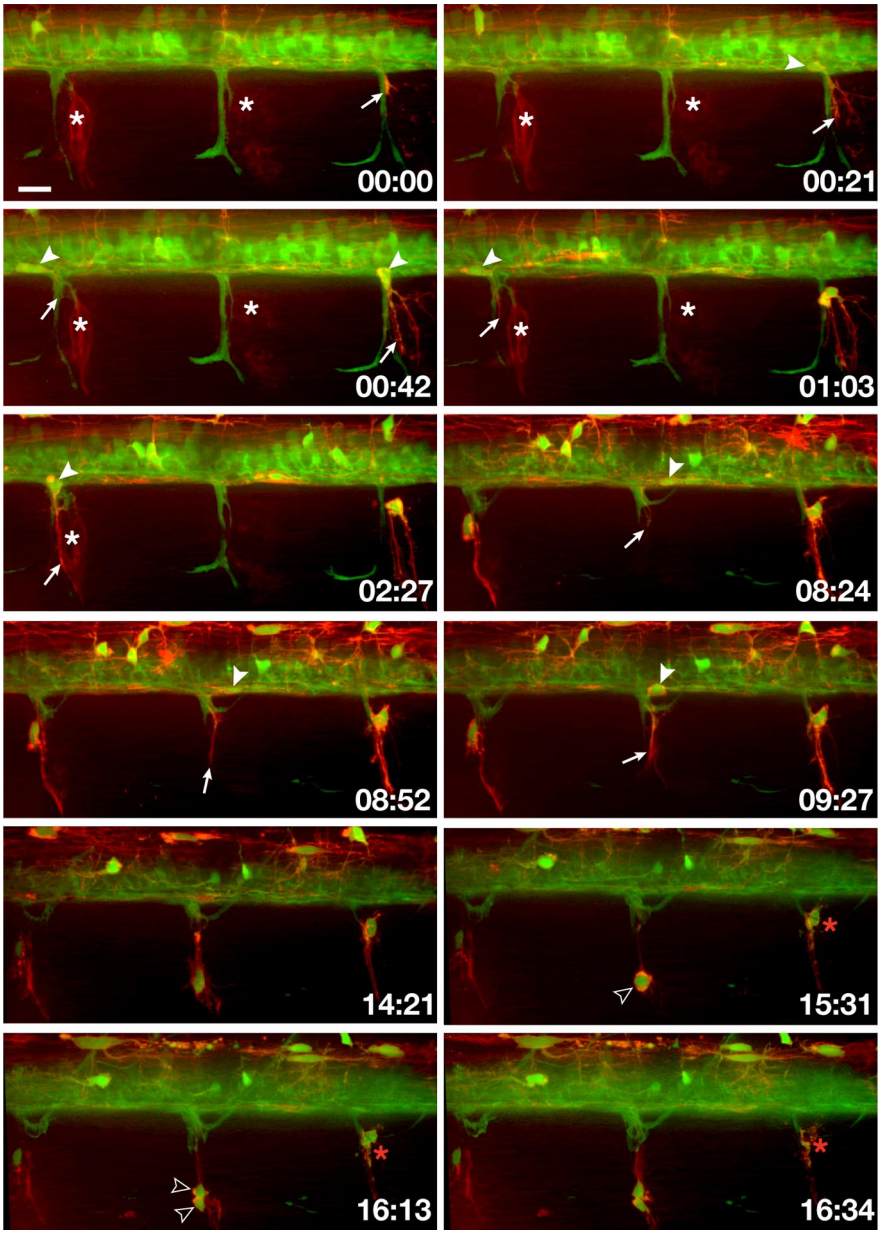

Figure 1. *In vivo*, time-lapse imaging shows that OPCs exit the spinal cord through MEPs in *cls*$^{-/-}$ larvae following Schwann cell death. Frames captured from a 24 h time-lapse sequence (supplemental Movie 2, available at www.jneurosci.org as supplemental material) of a *cls*$^{-/-}$*;Tg(olig2:egfp);Tg(sox10(7.2):mrfp)* larva beginning at 52 hpf. All images are lateral views at the level of the trunk spinal cord with dorsal to the top. Numbers in lower right corners denote time elapsed from the first frame of the figure. At ~55 hpf (00:00 time point), an *olig2*$^{+}$ *sox10*$^{+}$ OPC process (arrow) emerged from the ventral spinal cord along motor axons (green). Fragments of red membrane from Schwann cells that had recently died are visible in this frame. White asterisks mark clusters of Schwann cells that later fragment and die. As the sequence continues, white arrowheads mark OPC cell bodies within the spinal cord before their exit through MEPs and arrows mark their extending processes. OPCs often divided (open arrowheads) but eventually died (red asterisks). Scale bar, 12 μm.

nkx2.2^{+} or *nkx2.2*$^{-}$ (Kucenas et al., 2009). As we expected, neural crest deficient *mob*$^{-/-}$*;mos*$^{-/-}$*;Tg(nkx2.2a:megfp);Tg(sox10:mrfp)* larvae did not have Schwann cells (Fig. 3*A*; supplemental Movie 2, available at www.jneurosci.org as supplemental material). Perineurial glia extended processes from the spinal cord but did not migrate into the PNS, consistent with our previous observations that perineurial glia migration from the CNS requires the presence of Schwann cells (Kucenas et al., 2008). Instead, OPCs emerged from the spinal cord at each MEP. In contrast to *cls*$^{-/-}$ larvae, OPC cell bodies did not pause in the spinal cord after extending membrane processes through MEPs but emerged immediately after process extension. Similar to their behavior in *cls*$^{-/-}$ larvae, peripheral OPCs extended and retracted numerous membrane processes for several hours while they remained associated with motor nerves. Whereas peripheral OPCs eventually died in *cls*$^{-/-}$ larvae, extended periods of imaging revealed that OPCs wrapped motor axons in *mob*$^{-/-}$*;mos*$^{-/-}$ larvae (Fig. 3*B*; supplemental Fig. 1, supplemental Movie 3, both available at www.jneurosci.org as supplemental material). Notably, each OPC wrapped motor axons at multiple positions, a behavior characteristic of oligodendrocytes, instead of forming a single sheath like Schwann cells. Therefore, OPCs that exit the spinal cord in the absence of Schwann cells maintain their oligodendrocyte identity while they wrap motor axons.

OPCs ensheathe peripheral motor axons in *mob*$^{-/-}$*;mos*$^{-/-}$ larvae with CNS myelin

To learn whether oligodendrocytes can myelinate peripheral motor axons, we labeled larvae with an antibody that recognizes myelin basic protein (MBP). At 5 dpf, MBP was evident in spinal cord white matter, along motor nerve roots and at the lateral line nerve of wild-type larvae (Fig. 4*A*,*A*′) (data not shown). *mob*$^{-/-}$*;mos*$^{-/-}$ larvae similarly expressed MBP in spinal cord white matter (Fig. 4*B*), indicating that loss of Tfap2 and Foxd3 functions do not interfere with oligodendrocyte differentiation and myelination. In the periphery of mutant larvae, MBP expression was entirely absent from lateral line nerves (data not shown), consistent with the failure of Sox10^{+} cells to occupy the lateral line nerve. In contrast, anti-MBP labeled all ventral motor roots analyzed (Fig. 4*B*,*B*′), although the amount of MBP detected appeared less than in wild-type larvae (n = 12 larvae, ~10 motor roots/larva).

We further tested the ability of oligodendrocytes to myelinate peripheral motor axons using electron microscopy. At 5 dpf in wild-type larvae, Schwann cells formed multiple layers of loosely compacted myelin surrounding motor axons (Fig. 4*C*). Loosely compacted myelin was also apparent around motor axons in *mob*$^{-/-}$*;mos*$^{-/-}$ larvae (Fig. 4*D*) (n = 5 larvae, 10–12 motor roots/larvae), indicating that oligodendrocytes can undergo differentiation into functional myelinating glial cells in the PNS.

Schwann cells that invade the CNS produce myelin with peripheral characteristics (Gilmore et al., 1982; Sims and Gilmore, 1983). Therefore, we used gene expression to investigate whether motor-nerve associated oligodendrocytes form central or peripheral myelin in *mob*$^{-/-}$*;mos*$^{-/-}$ larvae. Oligodendrocytes but not Schwann cells express *proteolipid protein 1a (plp1a)* (Brösamle

and Halpern, 2002). As shown previously in wild-type larvae, *plp1a* expression was limited to oligodendrocytes that occupy ventral and dorsal spinal cord white matter (Fig. 5*A*,*B*). In contrast, *plp1a*$^{+}$ cells were periodically distributed along the trunk of *mob*$^{-/-}$;*mos*$^{-/-}$ larvae, just ventral to spinal cord, consistent with the distribution of peripheral oligodendrocytes (Fig. 5*C*,*D*).

OPC exit from spinal cord is not impeded by Boundary Cap cells in zebrafish

One possible explanation for our observations is that Schwann cells prevent OPC migration through MEPs. Alternatively, OPC migration from spinal cord in neural crest deficient mutant embryos might result from the absence of Boundary Cap (BC) cells, a transient, neural crest derived population that prevents motor neuron migration from the neural tube in bird and rodent embryos (Niederländer and Lumsden, 1996; Vermeren et al., 2003). Zebrafish BC cells have not been described. Therefore, we investigated expression of *egr2b*, also known as *krox20*, *cdh7*, *wif1*, *sema6d*, and *sema6 dl*, which are homologous to genes that mark BC cells in chick and mouse embryos (Niederländer and Lumsden, 1996; Vermeren et al., 2003; Coulpier et al., 2009). We did not detect expression of any gene that correlated with the positions of dorsal entry or ventral exit points (data not shown).

If zebrafish have neural crest-derived cells that are functionally equivalent to BC cells, then motor neurons should migrate from neural tube in embryos deficient for neural crest. Our time-lapse imaging of *cls*$^{-/-}$;*Tg(olig2:egfp):Tg(sox10(7.2):mrfp)* embryos, in which motor neurons express EGFP, did not reveal motor neuron exit from spinal cord (Fig. 1). We confirmed this using immunocytochemistry on transgenic, mutant embryos. We never found Isl^{+} Sox10^{-} cells, indicative of motor neurons, associated with motor roots in *cls* mutant embryos ($n = 12$ embryos) (supplemental Fig. 2, available at www.jneurosci.org as supplemental material). However, it is possible that the *cls/sox10* mutation does not interfere with BC cell function. Therefore, we also investigated the distribution of motor neurons in *mob;mos* mutant embryos using Isl immunocytochemistry. Double mutant embryos did not have peripheral Isl^{+} cells ($n = 7$ embryos) (supplemental Fig. 2, available at www.jneurosci.org as supplemental material) showing that, even in the absence of the entire neural crest population, motor neurons did not exit the spinal cord. These data indicate that, in zebrafish, a neural crest-derived BC population is not responsible for preventing motor neuron exit from the neural tube as in bird and rodent embryos. Therefore, OPC exit in normal development may be specifically blocked by interactions with Schwann cells at the CNS and PNS interface.

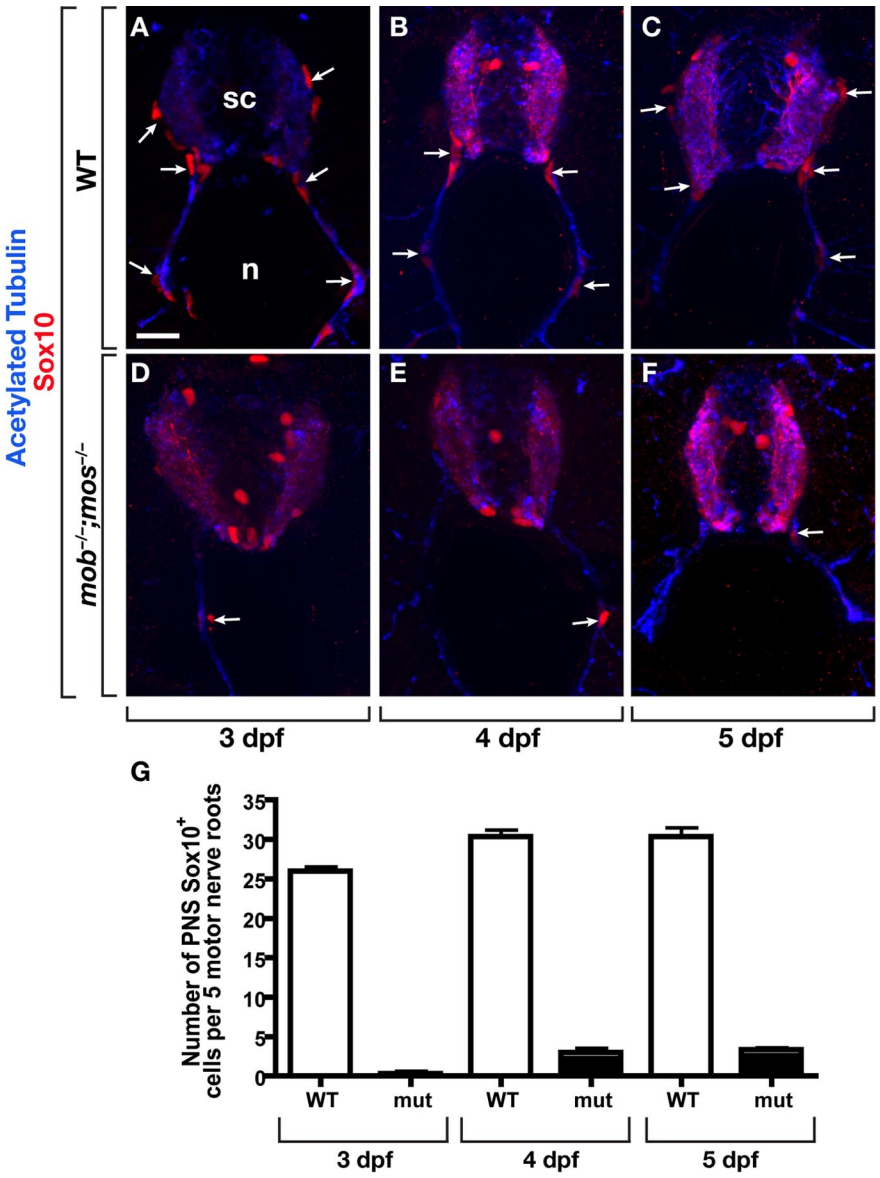

Figure 2. Sox10^{+} cells associate with motor roots in neural crest-deficient *mob*$^{-/-}$;*mos*$^{-/-}$ larvae. ***A–C***, Transverse sections, dorsal up, through the trunk of 3 (***A***), 4 (***B***), and 5 (***C***) dpf wild-type larvae labeled with antibodies to Sox10 (red) to mark Schwann cells and acetylated Tubulin (blue) to mark axons. Sox10^{+} Schwann cells (white arrows) are closely associated with dorsal and ventral motor roots. ***D–F***, *mob*$^{-/-}$;*mos*$^{-/-}$ larvae of the same ages have Sox10^{+} cells along motor roots, although there are fewer than in wild type. ***G***, Quantification of Sox10^{+} cells along ventral motor roots to the horizontal myoseptum. *mob*$^{-/-}$;*mos*$^{-/-}$ larvae at 3, 4 and 5 dpf had fewer cells than wild-type controls. sc, Spinal cord; n, notochord. Asterisks mark Sox10^{+} OPCs within the spinal cord. Scale bar, 24 μm.

Discussion

The outermost layer of the nerve cord is the glia limitans, consisting of an interwoven meshwork of radial glia and astrocyte membrane extensions covered by basal lamina. The glia limitans and basal lamina are altered at nerve entry and exits points, which serve as specialized transition zones between the CNS and PNS. Nerve root transition zones are morphologically diverse (Fraher, 1992) but generally feature a thickened glia limitans in which glial processes both surround the axon bundle at the point of attachment with the CNS and segregate individual axons (Fraher, 1992, 1997, 2000). The modified glia limitans of nerve root transition

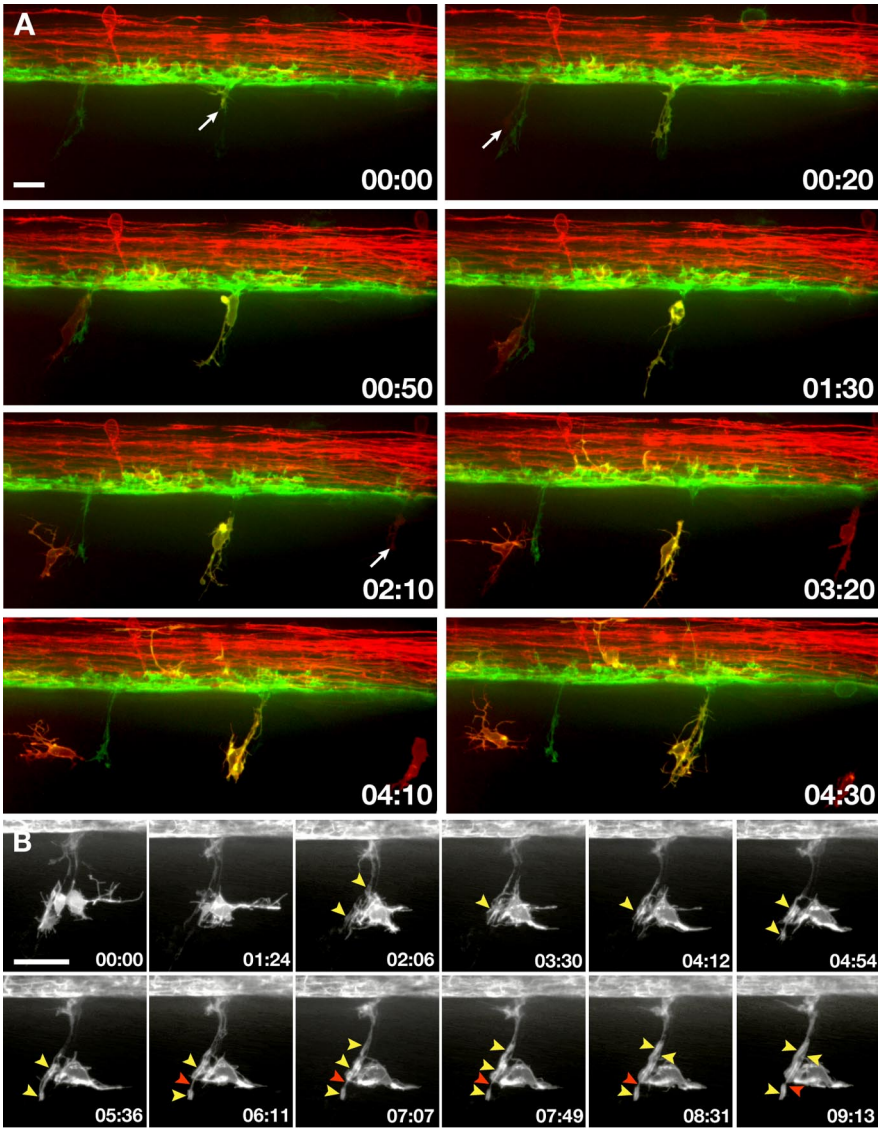

Figure 3. In the absence of Schwann cells, OPCs exit the spinal cord and wrap motor axons. All images present lateral views, dorsal up. Numbers in lower right corners denote time elapsed from first frame of the figure. ***A***, Frames captured from a 24 h time-lapse sequence (supplemental Movie 3, available at www.jneurosci.org as supplemental material) of a *mob* $^{-/-}$*;mos* $^{-/-}$*;Tg(nkx2.2a:megfp);Tg(sox10(7.2):mrfp)* larva beginning at 36 hpf. Several OPCs emerge from ventral spinal cord at regularly spaced intervals (arrows). ***B***, Frames captured from a 24 h time-lapse sequence (supplemental Movie 4, available at www.jneurosci.org as supplemental material) of a *mob* $^{-/-}$*;mos* $^{-/-}$*;Tg(nkx2.2a:megfp)* larva beginning at 62 hpf showing the behavior of a single OPC. As the sequence progresses, the OPC ensheathes motor axons with multiple processes (yellow arrowheads), which subsequently elongate. Red arrowhead marks nascent node between adjacent OPC processes. Scale bars: 12 μm (***A***), 24 μm (***B***).

zones could contribute to a selective barrier that permits axon extension but blocks the movement of neurons across the CNS–PNS interface.

Closely associated with nerve root transition zones during development of bird and rodent embryos are clusters of BC cells (Altman and Bayer, 1984; Wilkinson et al., 1989). BC cells arise from neural crest (Niederländer and Lumsden, 1996) and, after pausing at dorsal root entry zones, produce Schwann cells that associate with the dorsal root and neurons and satellite glia of the dorsal root ganglia (Maro et al., 2004). BC cells apparently cluster at transition zones before axons enter or exit the CNS (Niederländer and Lumsden, 1996; Vermeren et al., 2003), although another study concluded that BC cells arrive at motor axon exit points only after axons begin to emerge (Fraher et al., 2007). The close proximity of BC cells to transition zones raised the possibility that they determine the sites at which axons cross the CNS–PNS interface. However, heterotopic transplantation of hindbrain and spinal cord neural crest failed to provide supporting evidence (Niederländer and Lumsden, 1996). Therefore, the cues that position axon entry and exit points might arise solely within the neuroepithelium.

Another possible role for BC cells is that they are components of a selective barrier that regulates axon extension and neuronal migration across the CNS–PNS interface. Consistent with this, sensory axons preferentially extended over BC cells *in vitro* (Golding and Cohen, 1997). Motor axon extension, however, was unperturbed following surgical removal of neural crest and genetic ablation of BC cells (Vermeren et al., 2003), indicating that motor axon exit from the CNS does not require the presence of BC cells. Instead, motor axon cell bodies translocate along their axons to migrate from the CNS into the periphery (Vermeren et al., 2003), raising the possibility that BC cells inhibit movement of motor neuron cell bodies. Recent evidence revealed that Semophorin signaling, which plays numerous roles in axon guidance and cell migration, contributes at least partially to the mechanism that prevents motor neuron migration from the CNS. BC cells express the secreted Semaphorins Sema3b and Sema3G and membrane-bound Sema6A and Sema6D (Bron et al., 2007; Mauti et al., 2007; Coulpier et al., 2009), whereas motor neurons express PlexinA molecules (Mauti et al., 2007), which function as both ligands and receptors for class 6 Semaphorins (Tran et al., 2007), and Neuropilin1 (Npn1) and Npn2 coreceptors (Bron et al., 2007). One loss of function study indicated that Sema6A, Npn2, and PlexinA2, but not PlexinA1 functions are necessary to prevent motor neurons from leaving the CNS (Bron et al., 2007), whereas another study indicated that Sema6A and PlexinA1 are required (Mauti et al., 2007). Because Sema6a is bound to the cell membrane and BC cells are physically separated from motor neuron soma, the precise details of a Semaphorin-based gating mechanism remain unclear.

Whether zebrafish use a similar selective barrier mechanism at MEPs is still uncertain. *sema3a1* is expressed broadly throughout somites but does not seem to be enriched at nerve roots (Sato-Maeda et al., 2006). Zebrafish motor neurons express *plexina3* (Feldner et al., 2007; Palaisa and Granato, 2007; Tanaka et al., 2007) and the *Npn1* ortholog *nrp1a* (Bovenkamp et al., 2004; Yu et al., 2004; Feldner et al., 2005; Sato-Maeda et al., 2008). However, *plexina3* guides motor axon extension but is not required for motor neuron cell body retention in the spinal cord (Feldner

et al., 2007; Palaisa and Granato, 2007; Tanaka et al., 2007) and, whereas one study showed that some motor neurons appear to migrate from the spinal cord in the absence of *nrp1a* function (Feldner et al., 2005), another study did not find such evidence (Sato-Maeda et al., 2008). Furthermore, our own efforts thus far have uncovered neither gene expression nor functional evidence for BC cells in zebrafish. Instead, we recently showed that *nkx2.2a*$^{+}$ perineurial glial cells, which arise from ventral spinal cord and migrate through motor axon exit points to form motor nerve perineurium, prevent motor neuron exit from the spinal cord in zebrafish (Kucenas et al., 2008). We speculate that, before their migration, perineurial glia form a transient, selective barrier that allows motor axon projection but not cell body migration. We do not yet know the mechanism by which perineurial glia inhibit motor neuron exit.

It seems likely that the movement of glial cells across the CNS–PNS interface is also regulated. During development, OPCs arise from spatially restricted CNS precursors and migrate long distances to fill the neural tube. Similarly, Schwann cell progenitors are produced by neural crest, which forms at the dorsal neural tube, and migrate to, and along, peripheral axons. Despite these highly motile behaviors, oligodendrocyte and Schwann cell internodes come into close proximity on common axons without overlapping within nerve root transition zones (Fraher and Kaar, 1984). Schwann cells can be found in the CNS, but their presence in normal animals is very rare (Raine, 1976; Jung et al., 1978). Conversely, small islands of oligodendrocytes, usually associated with astrocytes, have been found in peripheral tissues of humans and macaques (Tarlov, 1937; Maxwell et al., 1969).

One possible impediment to glial migration across the CNS–PNS interface is the glia limitans and associated basal lamina. Consistent with this, large numbers of Schwann cells occupy spinal cord after damage to glial cells and the glia limitans by irradiation (Blakemore and Patterson, 1975; Gilmore et al., 1982; Sims and Gilmore, 1983; Sims et al., 1985) and following contusion injuries (Blight and Young, 1989; Beattie et al., 1997). Intriguingly, Schwann cells also can occupy the CNS in demyelination models and individuals affected by Multiple Sclerosis, even in the apparent absence of damage to the glia limitans (Ghatak et al., 1973; Raine et al., 1978; Itoyama et al., 1983, 1985; Yamamoto et al., 1991; Duncan and Hoffman, 1997). These latter observations raise the possibility that interactions between myelinating cells of the CNS and PNS reciprocally restrict their movements across the interface.

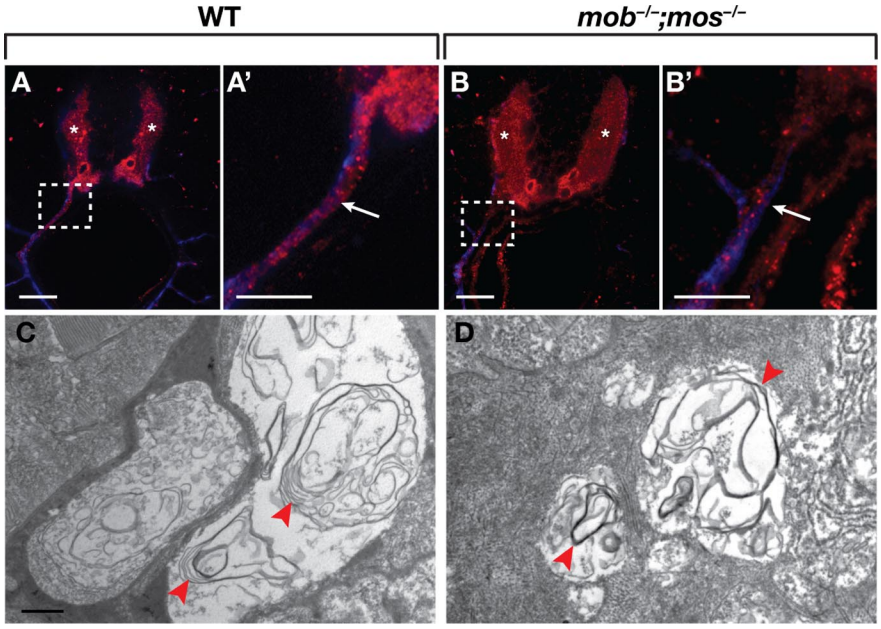

Figure 4. Oligodendrocytes myelinate motor axons in mutants lacking Schwann cells. ***A***, ***A′***, Transverse sections of a 5 dpf wild-type larva labeled with MBP (red) and acetylated Tubulin (blue) antibodies. MBP was present in the white matter of the spinal cord (asterisks) and along ventral motor roots (white arrow). ***B***, ***B′***, Transverse section of a 5 dpf *mob* $^{-/-}$;*mos* $^{-/-}$ larvae. Spinal cord expression of MBP was normal (white asterisks). MBP was also present along motor axons (arrow), although at reduced levels compared to wild type. ***A′*** and ***B′*** are enlarged views of the boxed regions in ***A*** and ***B***. ***C***, ***D***, Electron micrographs of motor nerves in wild-type (***C***) and *mob* $^{-/-}$;*mos* $^{-/-}$ (***D***) larvae at 5 dpf. Loosely compacted myelin surrounded motor axons in both wild type and mutant (red arrowheads). Scale bars: 24 μm (***A–B′***), 500 nm (***C***, ***D***).

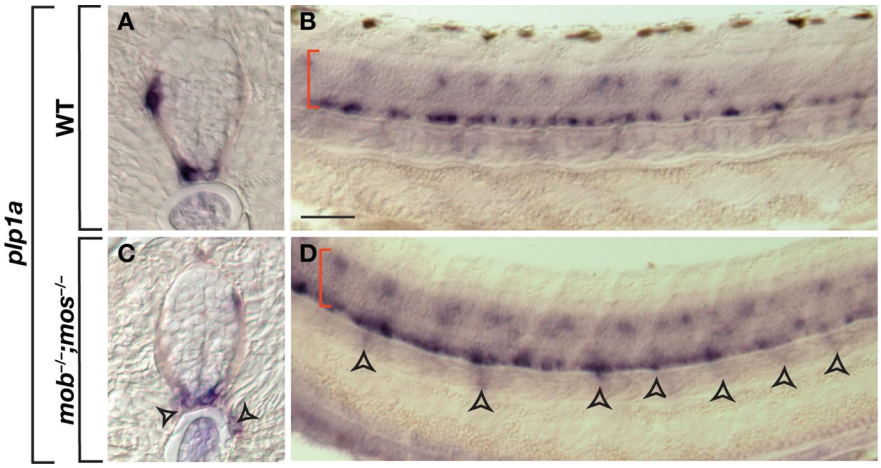

Figure 5. Oligodendrocytes maintain their identity in the periphery. ***A–D***, Transverse (***A***, ***C***) and whole mount (***B***, ***D***) views of *plp1a* expression in 3.5 dpf wild-type and *mob* $^{-/-}$;*mos* $^{-/-}$ larvae. Red brackets mark spinal cord. Arrowheads mark *plp1a* expression outside the spinal cord. Scale bar: 20 μm (***A***, ***C***), 50 μm (***B***, ***D***).

Our time-lapse imaging and genetic experiments now provide evidence that glial cell interactions contribute to the selective barrier mechanism that operates at nerve root transitional zones. In the absence of differentiated neural crest derivatives or following Schwann cell death, OPCs migrated through MEPs, wrapped motor axons at multiple positions, consistent with oligodendrocyte behavior, and produced CNS myelin. We previously showed that OPCs dynamically interact during development and that OPCs divide, migrate and wrap axons following ablation of oligodendrocytes with a laser (Kirby et al., 2006), which suggests that interactions between OPCs influence their number and spacing within the CNS. We propose that a similarly simple

mechanism operates to selectively limit glial cell movement across the CNS–PNS interface. Under normal circumstances, OPC-Schwann cell interactions at nerve root transition zones block their movements across the interface. However, if no Schwann cell or Schwann cell-derived signal is encountered, OPCs can migrate out of the CNS along peripheral axons and myelinate them. Notably, the interactions are specific to myelinating cells because perineurial glia migrate through motor axon exit points in the presence of Schwann cells (Kucenas et al., 2008).

In summary, our work provides evidence that the transition between CNS and PNS myelin on axons that cross the interface is established by interactions between myelinating glia. During development, these interactions might serve to limit OPC movement across the interface, but not that of Schwann cells, because Schwann cells arrive at motor axons before OPCs are born. Therefore, it will be important to identify the mechanism of Schwann cell exclusion from the developing neural tube to fully understand how myelinating cells remain segregated within different compartments. One implication of our observations is that the ability of OPCs to cross the interface in the absence of Schwann cells might contribute to myelin homeostasis whereby perturbations that result in a deficit of Schwann cells are compensated by OPC migration from the spinal cord. Our work also raises a question about the functional significance of separating myelinating cell populations and whether failures to do so impair peripheral nerve function or contribute to peripheral nerve disease.

References

Altman J, Bayer SA (1984) The development of the rat spinal cord. Adv Anat Embryol Cell Biol 85:1–164.

Arduini BL, Bosse KM, Henion PD (2009) Genetic ablation of neural crest cell diversification. Development 136:1987–1994.

Barrallo-Gimeno A, Holzschuh J, Driever W, Knapik EW (2004) Neural crest survival and differentiation in zebrafish depends on mont blanc/tfap2a gene function. Development 131:1463–1477.

Beattie MS, Bresnahan JC, Komon J, Tovar CA, Van Meter M, Anderson DK, Faden AI, Hsu CY, Noble LJ, Salzman S, Young W (1997) Endogenous repair after spinal cord contusion injuries in the rat. Exp Neurol 148:453–463.

Bhattacharyya A, Brackenbury R, Ratner N (1994) Axons arrest the migration of Schwann cell precursors. Development 120:1411–1420.

Blakemore WF, Patterson RC (1975) Observations on the interactions of Schwann cells and astrocytes following X-irradiation of neonatal rat spinal cord. J Neurocytol 4:573–585.

Blight AR, Young W (1989) Central axons in injured cat spinal cord recover electrophysiological function following remyelination by Schwann cells. J Neurol Sci 91:15–34.

Bovenkamp DE, Goishi K, Bahary N, Davidson AJ, Zhou Y, Becker T, Becker CG, Zon LI, Klagsbrun M (2004) Expression and mapping of duplicate neuropilin-1 and neuropilin-2 genes in developing zebrafish. Gene Expr Patterns 4:361–370.

Bron R, Vermeren M, Kokot N, Andrews W, Little GE, Mitchell KJ, Cohen J (2007) Boundary cap cells constrain spinal motor neuron somal migration at motor exit points by a semaphorin-plexin mechanism. Neural Dev 2:21.

Brösamle C, Halpern ME (2002) Characterization of myelination in the developing zebrafish. Glia 39:47–57.

Coulpier F, Le Crom S, Maro GS, Manent J, Giovannini M, Maciorowski Z, Fischer A, Gessler M, Charnay P, Topilko P (2009) Novel features of boundary cap cells revealed by the analysis of newly identified molecular markers. Glia 57:1450–1457.

Duncan ID, Hoffman RL (1997) Schwann cell invasion of the central nervous system of the myelin mutants. J Anat 190:35–49.

Dutton KA, Pauliny A, Lopes SS, Elworthy S, Carney TJ, Rauch J, Geisler R, Haffter P, Kelsh RN (2001) Zebrafish colourless encodes sox10 and specifies non-ectomesenchymal neural crest fates. Development 128:4113–4125.

Feldner J, Becker T, Goishi K, Schweitzer J, Lee P, Schachner M, Klagsbrun M, Becker CG (2005) Neuropilin-1a is involved in trunk motor axon outgrowth in embryonic zebrafish. Dev Dyn 234:535–549.

Feldner J, Reimer MM, Schweitzer J, Wendik B, Meyer D, Becker T, Becker CG (2007) PlexinA3 restricts spinal exit points and branching of trunk motor nerves in embryonic zebrafish. J Neurosci 27:4978–4983.

Fraher JP (1992) The CNS-PNS transitional zone of the rat. Morphometric studies at cranial and spinal levels. Prog Neurobiol 38:261–316.

Fraher JP (1997) Axon-glial relationships in early CNS-PNS transitional zone development: an ultrastructural study. J Neurocytol 26:41–52.

Fraher JP (2000) The transitional zone and CNS regeneration. J Anat 196:137–158.

Fraher JP, Kaar GF (1984) The transitional node of Ranvier at the junction of the central and peripheral nervous systems: an ultrastructural study of its development and mature form. J Anat 139:215–238.

Fraher JP, Dockery P, O'Donoghue O, Riedewald B, O'Leary D (2007) Initial motor axon outgrowth from the developing central nervous system. J Anat 211:600–611.

Ghatak NR, Hirano A, Doron Y, Zimmerman HM (1973) Remyelination in multiple sclerosis with peripheral type myelin. Arch Neurol 29:262–267.

Gilmore SA, Sims TJ (1997) Glial-glial and glial-neuronal interfaces in radiation-induced, glia-depleted spinal cord. J Anat 190:5–21.

Gilmore SA, Sims TJ, Heard JK (1982) Autoradiographic and ultrastructural studies of areas of spinal cord occupied by Schwann cells and Schwann cell myelin. Brain Res 239:365–375.

Golding JP, Cohen J (1997) Border controls at the mammalian spinal cord: late-surviving neural crest boundary cap cells at dorsal root entry sites may regulate sensory afferent ingrowth and entry zone morphogenesis. Mol Cell Neurosci 9:381–396.

Itoyama Y, Webster HD, Richardson EP Jr, Trapp BD (1983) Schwann cell remyelination of demyelinated axons in spinal cord multiple sclerosis lesions. Ann Neurol 14:339–346.

Itoyama Y, Ohnishi A, Tateishi J, Kuroiwa Y, Webster HD (1985) Spinal cord multiple sclerosis lesions in Japanese patients: Schwann cell remyelination occurs in areas that lack glial fibrillary acidic protein (GFAP). Acta Neuropathol 65:217–223.

Jung HJ, Raine CS, Suzuki K (1978) Schwann cells and peripheral nervous system myelin in the rat retina. Acta Neuropathol 44:245–247.

Kalderon N (1979) Migration of Schwann cells and wrapping of neurites in vitro: a function of protease activity (plasmin) in the growth medium. Proc Natl Acad Sci U S A 76:5992–5996.

Kirby BB, Takada N, Latimer AJ, Shin J, Carney TJ, Kelsh RN, Appel B (2006) In vivo time-lapse imaging shows dynamic oligodendrocyte progenitor behavior during zebrafish development. Nat Neurosci 9:1506–1511.

Kucenas S, Takada N, Park HC, Woodruff E, Broadie K, Appel B (2008) CNS-derived glia ensheath peripheral nerves and mediate motor root development. Nat Neurosci 11:143–151.

Kucenas S, Snell H, Appel B (2009) nkx2.2a promotes specification and differentiation of a myelinating subset of oligodendrocyte lineage cells. Neuron Glia Biol 4:71–81.

Maro GS, Vermeren M, Voiculescu O, Melton L, Cohen J, Charnay P, Topilko P (2004) Neural crest boundary cap cells constitute a source of neuronal and glial cells of the PNS. Nat Neurosci 7:930–938.

Mauti O, Domanitskaya E, Andermatt I, Sadhu R, Stoeckli ET (2007) Semaphorin6A acts as a gate keeper between the central and the peripheral nervous system. Neural Dev 2:28.

Maxwell DS, Kruger L, Pineda A (1969) The trigeminal nerve root with special reference to the central-peripheral transition zone: an electron microscopic study in the macaque. Anat Rec 164:113–125.

Montero-Balaguer M, Lang MR, Sachdev SW, Knappmeyer C, Stewart RA, De La Guardia A, Hatzopoulos AK, Knapik EW (2006) The mother superior mutation ablates foxd3 activity in neural crest progenitor cells and depletes neural crest derivatives in zebrafish. Dev Dyn 235:3199–3212.

Neuhauss SC, Solnica-Krezel L, Schier AF, Zwartkruis F, Stemple DL, Malicki J, Abdelilah S, Stainier DY, Driever W (1996) Mutations affecting craniofacial development in zebrafish. Development 123:357–367.

Niederländer C, Lumsden A (1996) Late emigrating neural crest cells migrate specifically to the exit points of cranial branchiomotor nerves. Development 122:2367–2374.

Palaisa KA, Granato M (2007) Analysis of zebrafish sidetracked mutants reveals a novel role for Plexin A3 in intraspinal motor axon guidance. Development 134:3251–3257.

Park HC, Boyce J, Shin J, Appel B (2005) Oligodendrocyte specification in

zebrafish requires notch-regulated cyclin-dependent kinase inhibitor function. J Neurosci 25:6836–6844.

Raine CS (1976) On the occurrence of Schwann cells within the normal central nervous system. J Neurocytol 5:371–380.

Raine CS, Traugott U, Stone SH (1978) Glial bridges and Schwann cell migration during chronic demyelination in the C.N.S. J Neurocytol 7:541–553.

Sato-Maeda M, Tawarayama H, Obinata M, Kuwada JY, Shoji W (2006) Sema3a1 guides spinal motor axons in a cell- and stage-specific manner in zebrafish. Development 133:937–947.

Sato-Maeda M, Obinata M, Shoji W (2008) Position fine-tuning of caudal primary motoneurons in the zebrafish spinal cord. Development 135:323–332.

Shin J, Park HC, Topczewska JM, Mawdsley DJ, Appel B (2003) Neural cell fate analysis in zebrafish using olig2 BAC transgenics. Methods Cell Sci 25:7–14.

Sims TJ, Gilmore SA (1983) Interactions between intraspinal Schwann cells and the cellular constituents normally occurring in the spinal cord: an ultrastructural study in the irradiated rat. Brain Res 276:17–30.

Sims TJ, Gilmore SA, Waxman SG, Klinge E (1985) Dorsal-ventral differences in the glia limitans of the spinal cord: an ultrastructural study in developing normal and irradiated rats. J Neuropathol Exp Neurol 44:415–429.

Tanaka H, Maeda R, Shoji W, Wada H, Masai I, Shiraki T, Kobayashi M, Nakayama R, Okamoto H (2007) Novel mutations affecting axon guidance in zebrafish and a role for plexin signalling in the guidance of trigeminal and facial nerve axons. Development 134:3259–3269.

Tarlov IM (1937) Structure of the nerve root. I. Nature of the junction between the central and the peripheral nervous system. Arch Neurol Psych 37:555–583.

Tran TS, Kolodkin AL, Bharadwaj R (2007) Semaphorin regulation of cellular morphology. Annu Rev Cell Dev Biol 23:263–292.

Vermeren M, Maro GS, Bron R, McGonnell IM, Charnay P, Topilko P, Cohen J (2003) Integrity of developing spinal motor columns is regulated by neural crest derivatives at motor exit points. Neuron 37:403–415.

Wilkinson DG, Bhatt S, Chavrier P, Bravo R, Charnay P (1989) Segment-specific expression of a zinc-finger gene in the developing nervous system of the mouse. Nature 337:461–464.

Yamamoto T, Kawamura J, Hashimoto S, Nakamura M (1991) Extensive proliferation of peripheral type myelin in necrotic spinal cord lesions of multiple sclerosis. J Neurol Sci 102:163–169.

Yu HH, Houart C, Moens CB (2004) Cloning and embryonic expression of zebrafish neuropilin genes. Gene Expr Patterns 4:371–378.